APPROXIMATE SOLUTIONS OF RADIATIVE TRANSFER IN ONE-DIMENSIONAL NON-PLANAR SYSTEMS

W. W. YUEN† and C. L. TIEN

Department of Mechanical Engineering. University of California. Berkeley, CA 94720, U.S.A.

Abstract—An approximate method is developed for the study of radiative transfer in one-dimensional. non-planar systems. While this method can be regarded as an extension of some existing approximation techniques formulated for the one-dimensional planar problem. it does yield closed-form expressions for the radiant heat flux and the temperature profile for various non-planar problems. which have not been established before. Comparisons with the available numerical results show that the heat-flux expressions are accurate throughout the entire range of the optical thickness. Results for the temperature profile. however. have the same limitation as the various closed-form approximate solutions for the planar problem. They are not very accurate at regions near the boundary. except in the optically thick limit. Based on the closed-form expressions obtained for the non-planar radiative transfer problem. the present work establishes readily the effect of the various parameters. such as the optical thickness. the surface emissivity. the radius ratio and the heat-generation rate on the heat-transfer and the temperature profile. Differences between radiative heat-transfer characteristics of the two basic non-planar systems (concentric cylinders and concentric spheres) are discussed.

1. INTRODUCTION

COMPARED to the problem of radiative transfer in a one-dimensional planar medium, radiative transfer in systems with cylindrical or spherical geometries has received very little attention despite its practical significance. The major difficulty of the non-planar radiative transfer problem lies in its great theoretical complexity. Solution techniques, which were successful in obtaining the exact solution for the one-dimensional planar problem, are shown to be extremely complicated when applied to the non-planar problem.[1-3] Many of the existing approximation methods, such as the diffusion approximation,[4] the moment method[5] and the differential approximation,[6] which yield accurate heat-flux predictions for the one-dimensional planar problem, are not directly applicable to the non-planar problem. All of these approximation methods give inaccurate heat flux predictions in the optically thin limit. Numerically, computation for the non-planar radiative transfer problem is a very formidable task. In separate independent studies, RYHMING[7] and USISKIN et al.[8] solved the problem of radiative equilibrium in a concentric spherical enclosure utilizing a direct numerical integration technique. Their results show that the computation can be quite tedious and lengthy because the governing equation for radiative transfer is singular and generally not well suited for a direct numerical integration. HOWELL and PERLMUTTER[9] applied the Monte Carlo technique to the problem of radiative equilibrium in a concentric cylindrical enclosure. But their success is also quite limited because the computation can become very lengthy in the optically thick limit and inaccurate in the optically thin limit. Extensive parametric study of the non-planar radiative transfer problem based on these numerical computations seems very difficult and impractical.

The objective of the present work is to develop an approximate solution for the non-planar radiative transfer problem which is applicable for all values of the optical thickness. Utilizing results of the existing approximations[4,10] for the one-dimensional planar problem and a differential formulation of the radiation intensity recently developed,[10] closed-form expressions for the radiant heat flux and the temperature profile for problems of radiative transfer in a concentric cylindrical enclosure and a concentric spherical enclosure (both with and without heat generation) are obtained. Comparing with the existing numerical solutions,[7-9] the various heat flux expressions are shown to be quite accurate throughout the entire range of the optical thickness. The accuracy of the various temperature profiles is less satisfactory. Similar to

†Present address; Department of Mechanical and Environmental Engineering, University of California, Santa Barbara, CA 93106, U.S.A.

results of the many existing approximations for the one-dimensional planar problem, temperature profiles developed in this work are generally not very accurate near the two boundaries, except in the optically thick limit.

Based on these closed-form approximate expressions, the present work establishes readily the effect of the various physical parameters such as the surface emissivity, the optical thickness and the radius ratio on the heat transfer and temperature profile results for the two considered non-planar radiative transfer problems. The radiative heat transfer characteristics of the concentric cylindrical enclosure and that of the concentric spherical enclosure are also compared and discussed.

2. PHYSICAL MODEL

The present work deals with the problem of one-dimensional radiative transfer in enclosures with non-planar geometry neglecting the effect of conduction. Two particular geometries are considered, concentric cylinders and concentric spheres. For simplicity, the two boundaries are assumed to be isothermal, gray, diffusely emitting and reflecting surfaces of the same emissivity. The space between the two surfaces is assumed to be filled with an isotropic, homogeneous, absorbing and emitting medium with a constant absorption coefficient and uniform heat generation. Since these problems have no angular dependence, coordinate systems for the two considered geometries are identical. They are illustrated in Fig. 1.

With no angular dependence, the governing equation for the one-dimensional non-planar radiative transfer problem is the following familiar energy conservation relation:

$$\frac{d}{dr}[Q_r r^n] = S r^n. \tag{1}$$

where r is the radial coordinate, Q_r the radiant heat flux in the radial direction and S the internal heat generation rate. By setting $n = 1$ for the concentric-cylinders problem and $n = 2$ for the concentric-spheres problem, eqn (1) is applicable to both non-planar cases.

Utilizing the radiative transfer equation[2,3] and the differential formulation of the radiation intensity,[10] eqn (1) can be rewritten in the following form in terms of the gas temperature:

$$\sum_{k=0}^{\infty} \left(\frac{4}{2k+3}\right) \frac{1}{a^{2k+2}} [\nabla^{2(k+1)}(\sigma T^4)] = -\frac{S}{a}, \tag{2}$$

where a is the absorption coefficient, σ the Stefan–Boltzman constant, T the gas temperature and ∇^2 is the Laplacian operator defined as

$$\nabla^2 = \frac{1}{r^n} \frac{d}{dr}\left[r^n \frac{d}{dr}\right] \tag{3}$$
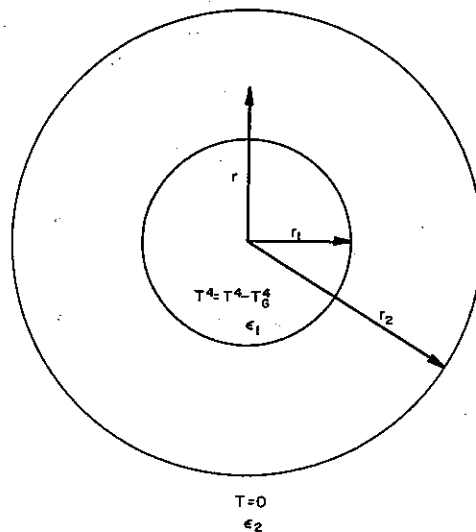

Fig. 1. Coordinate system for the one-dimensional non-planar problem.

with $n = 1$ for the case with the concentric cylinders and $n = 2$ for the case with the concentric spheres.

Introducing the dimensionless variables

$$q = Q_r/\sigma T_1^4, \quad \theta = T/T_1, \quad \rho = ar,$$
$$\nabla_\rho^2 = (1/a^2)/\nabla^2, \quad T_G^4 = S/a\sigma, \quad \theta_G = T_G/T_1, \tag{4}$$

where T_1 is the reference temperature defined in Fig. 1, eqns (1) and (2) can be rewritten in the following dimensionless form

$$\frac{d}{d\rho}[q\rho^n] = \theta_G^4 \rho^n. \tag{1a}$$

$$\sum_{k=0}^{\infty} \left(\frac{4}{2k+3}\right)[\nabla_\rho^{2(k+1)}\theta^4] = \theta_G^4. \tag{2a}$$

The boundary condition for eqn (2a) is the intensity boundary condition or, for the differential formulation, the multi-moment boundary condition.[10] It is interesting to observe that, by choosing the boundary condition to be $T^4 = T_1^4 - T_G^4$ at the inner wall and $T^4 = 0$ at the outer wall as shown in Fig. 1, the two solutions obtained by setting $T_G = T_1$ and $T_G = 0$ represent the two fundamental solutions of the one-dimensional non-planar problem. The solution to the problem with arbitrary surface temperatures and heat generation rates can be constructed by superposition of these solutions.

As was mentioned, an exact solution to the one-dimensional non-planar radiative transfer is quite difficult to obtain. The current work presents an approximate analysis.

3. APPROXIMATE SOLUTIONS

Radiative transfer between two concentric cylinders

Limiting solution. In the limit of $r_1/r_2 \to 1.0$, where r_1 and r_2 are, respectively, the radius of the inner surface and the radius of the outer surface, the problem of radiative transfer in a concentric cylindrical enclosure becomes identical to the one-dimensional planar problem. The curvature effect is negligibly small. The governing equation and boundary conditions at the two boundary surfaces are reduced to those for the planar case. To obtain an approximate solution for the concentric cylinders problem when the value of r_1/r_2 is close to unity, the existing approximation techniques[4,10] for the planar problem can clearly be applied.

Consider the case with no internal heat generation ($\theta_G = 0$); the success of the existing approximate solutions[4,10] for the one-dimensional planar problem suggests that the temperature profile within the concentric cylindrical enclosure can be written as

$$\theta^4 = \lambda + \beta\rho. \tag{5}$$

The heat-flux expression, neglecting the curvature effect, becomes[10]

$$q = -\frac{4}{3}\frac{d\theta^4}{d\rho} - \frac{4}{5}\frac{d^3\theta^4}{d\rho^3} - \cdots \tag{6}$$

At $r = r_1$ and $r = r_2$, the radiant-heat fluxes at the two cylindrical boundaries are

$$q(r_2) = -\frac{4}{3}\beta. \tag{7}$$

$$q(r_1) = -\frac{4}{3}\beta(r_2/r_1), \tag{8}$$

where the energy conservation relation has been used to obtain eqn (8). The two parameters λ and β can be obtained by observing the heat-flux boundary condition. Utilizing the differential formulation,[10] this boundary condition is

$$q(r_1) = \epsilon_1\left[1 - \theta^4 - \frac{2}{3}\frac{d\theta^4}{d\rho} - \frac{1}{4}\frac{d^2\theta^4}{d\rho^2} - \cdots\right]_{r=r_1}. \tag{9}$$

$$q(r_2) = \epsilon_2\left[\theta^4 - \frac{2}{3}\frac{d\theta^4}{d\rho} + \frac{1}{4}\frac{d^2\theta^4}{d\rho^2} - \cdots\right]_{r=r_2}. \tag{10}$$

where ϵ_1 and ϵ_2 are the inner surface emissivity and the outer surface emissivity, respectively. Substituting eqns (5), (7) and (8) into eqns (9) and (10) yields the following relations:

$$-\frac{4}{3\epsilon_1}\frac{\beta}{D} = 1 - \lambda - \beta\rho_1 - \frac{2}{3}\beta, \tag{11}$$

$$-\frac{4}{3\epsilon_2}\beta = \lambda + \beta\rho_2 - \frac{2}{3}\beta, \tag{12}$$

where $D = r_1/r_2$, $\rho_1 = ar_1$ and $\rho_2 = ar_2$. Solution to eqns (11) and (12) can be easily obtained. Limiting approximate expressions for the heat loss from the inner cylinder and the temperature profile are given by

$$q_r(r_1) = \frac{1}{1/\epsilon_1 \phi D\left(\frac{1}{\epsilon_2} - 1\right) + \frac{3}{4}D\rho_{12}}, \tag{13}$$

$$\theta^4 = \frac{\frac{4}{3\epsilon_2} - \frac{2}{3} + \rho_2 - \rho}{\frac{4}{3\epsilon_1}D + \frac{4}{3\epsilon_2} - \frac{4}{3} + \rho_{12}}, \tag{14}$$

where $\rho_{12} = \rho_2 - \rho_1$. But, because of the $D \to 1$ assumption, the application of eqns (13) and (14) is quite limited.

General solution. The important advantage of the above limiting approximate solution is that it can be easily generalized to obtain a solution for an enclosure with arbitrary values of D. Physically, a concentric cylindrical enclosure can be subdivided into many cylindrical subsections with infinitesimal thickness. The ratio of the inner radius to the outer radius for each subsection is effectively unity and the above approximation procedure can then be applied. By combining solutions for the different subsections, an approximate solution which is applicable for all values of D can be constructed.

To illustrate the generalized approximation procedure mathematically, consider the subdivision of the enclosure into n sections as shown in Fig. 2. The temperature profile is assumed to be represented by n distinct linear expressions as follows:

$$\theta^4 = \lambda_\nu + \beta_\nu\rho, \quad \rho_1 + \frac{(\nu - 1)}{n}\rho_{12} \leq \rho \leq \rho_1 + \frac{\nu\rho_{12}}{n}, \tag{15}$$

with $\nu = 1, 2, \ldots, n$. The values of λ_ν and β_ν can be obtained by observing the heat-flux conservation condition at all of the $(n + 1)$ boundaries and the temperature-continuity condition at the $(n - 1)$ boundaries away from the two cylindrical surfaces.

At the surface of the two cylinders, the heat-flux boundary condition is represented by the
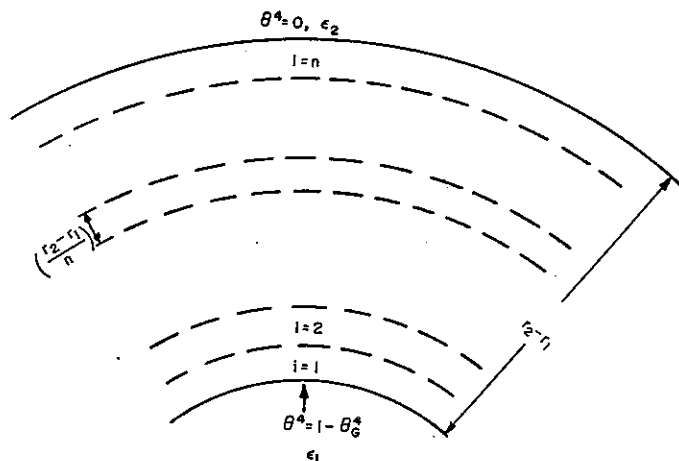

Fig. 2. Subdivision of the non-planar enclosure into n sections for the generalized approximate solution.

following pair of expressions which are similar to eqns (11) and (12):

$$-\frac{4}{3\epsilon_1}\beta_1 = 1 - \lambda_1 - \beta_1\rho_1 - \frac{2}{3}\beta_1, \tag{16}$$

$$-\frac{4}{3\epsilon_2}\beta_n \frac{\left(\rho_2 - \frac{\rho_{12}}{n}\right)}{\rho_2} = \lambda_n + \beta_n\rho_2 - 2/3\beta_n. \tag{17}$$

As in eqn (11), the left-hand side of eqn (17) is the result of the energy-conservation condition at the nth section.

At the remaining $(n-1)$ boundaries away from the two cylinders, it is necessary to consider the heat-flux condition between two adjacent layers of gas. Again utilizing the differential formulation,[10] the general expression for this boundary condition can be written as

$$q_r\left(\rho_1 + \frac{\nu\rho_{12}}{n}\right) = \left[\int_\Omega i_+ l_r \, d\Omega + \int_\square i_- l_r \, d\Omega\right]_{\rho = \rho_1 + (\nu\rho_{12}/n)}, \tag{18}$$

with

$$i_+ = \left[\theta^4 - \frac{\partial\theta^4}{\partial r} l_r + \cdots\right]_{\rho_1 + ((\nu-1)/n)\rho_{12} \leq \rho \leq \rho_1 + (\nu/n)\rho_{12}},$$

$$i_- = \left[\theta^4 - \frac{\partial\theta^4}{\partial r} l_r + \cdots\right]_{\rho_1 + (\nu/n)\rho_{12} \leq \rho \leq \rho_1 + ((\nu+1)/n)\rho_{12}},$$

where $d\Omega$ is the differential solid angle, l_r the directional cosine in the radial direction and $\nu = 1, 2, \ldots, n-1$. In terms of the unknown coefficients λ_ν and β_ν, eqns (18) become

$$-\frac{4}{3}\beta_\nu \frac{\rho_1 + (\nu-1)\frac{\rho_{12}}{n}}{\rho_1 + (\nu/n)\rho_{12}} = \lambda_\nu + \beta_\nu\left(\rho_1 + \frac{\nu\rho_{12}}{n}\right) - \frac{2}{3}\beta_\nu - \lambda_{\nu+1}$$

$$-\beta_{\nu+1}\left(\rho_1 + \frac{\rho_{12}}{n}\right) - \frac{2}{3}\beta_{\nu+1}, \tag{19}$$

with $\nu = 1, 2, \ldots, n-1$. But, physically, the gas temperature is continuous across the boundary between the two identical layers of gas. It requires

$$\lambda_\nu + \beta_\nu\left(\rho_1 + \frac{\rho_{12}}{n}\right) + \lambda_{\nu+1} + \beta_{\nu+1}\left(\rho_1 + \frac{\rho_{12}}{n}\right) \tag{20}$$

for all values of ν. Equation (19) can then be simplified to

$$-\frac{4}{3}\beta_\nu \frac{\rho_1 + (\nu-1)\frac{\rho_{12}}{n}}{\rho_1 + (\nu/n)\rho_{12}} = -\frac{2}{3}\beta_\nu - \frac{2}{3}\beta_{\nu+1} \tag{21}$$

with $\nu = 1, 2, \ldots, n-1$.

In the limit of $n \to \infty$, a simple addition of the $(n+1)$ boundary conditions represented by eqns (16), (17) and (21) yields the following relation:

$$-\frac{4}{3\epsilon_1}\beta_1 + \frac{4}{3}\beta_1 - \frac{4}{3\epsilon_2}\beta_n = 1 - \lambda_1 + \lambda_n - \beta_1\rho_1 + \beta_n\rho_2. \tag{22}$$

It is interesting to observe that eqn (22) involves only the approximate temperature profile at sections adjacent to the two cylindrical surfaces. To relate the four unknown coefficients λ_1, β_1, λ_n and β_n further in eqn (22), the temperature-continuity condition at the boundary between adjacent gas layers and the conservation of energy within each subsection are considered in the limit of large n.

For large value of n, the two unknown coefficients at each subsection can be treated as continuous functions, $\lambda(\rho)$ and $\beta(\rho)$. The temperature-continuity condition, represented by eqn (2) when n is finite, takes the following differential form:

$$\lambda(\rho) + \beta(\rho)\rho = \lambda(\rho + d\rho) + \beta(\rho + d\rho)\rho. \tag{23}$$

Expanding $\lambda(\rho + d\rho)$ and $\beta(\rho + d\rho)$ by Taylor's series and taking the limit with $d\rho \to 0$, eqn (23) is reduced to

$$\frac{d\lambda}{d\rho} + \frac{d\beta}{d\rho}\rho = 0. \tag{24}$$

By a similar argument, the conservation of energy within each infinitesimal subsection, which is utilized to obtain the left-hand side of eqns (17) and (21), can be expressed as

$$\frac{d}{dr}\left[-\frac{4}{3}\beta(\rho)r \right] = 0. \tag{25}$$

Equations (24) and (25) can be easily integrated to obtain

$$\lambda(\rho) = \lambda_n + \beta_n\rho_2 \ln\left(\frac{\rho}{\rho_2}\right) - \beta_n\rho_m, \tag{26}$$

$$\beta(\rho) = \beta_n\left(\frac{\rho_2}{\rho}\right), \tag{27}$$

where $\rho_m = (\rho_1 + \rho_2)/2$, $\lambda_n = \lambda(\rho_2)$ and $\beta_n = \beta(\rho_2)$. Evaluating eqns (26) and (27) at the inner cylinder and substituting into eqn (22) and (17), solutions for λ_n and β_n are readily obtained. These are

$$\beta_n = \frac{1}{-\dfrac{4}{3\epsilon_2} + \dfrac{4}{3} - \dfrac{4}{3\epsilon_1 D} + \left(\dfrac{\ln D}{1-D}\right)\rho_{12}}, \tag{28}$$

$$\lambda_n = \frac{-\dfrac{\rho_{12}}{2} - \dfrac{4}{3\epsilon_2} + \dfrac{2}{3}}{-\dfrac{4}{3\epsilon_2} + \dfrac{4}{3} - \dfrac{4}{3\epsilon_1 D} + \left(\dfrac{\ln D}{1-D}\right)\rho_{12}}. \tag{29}$$

The heat loss from the inner cylinder and the temperature profile within the enclosure, based on this generalized approximation procedure, become

$$q_r(r_1) = \frac{1}{\dfrac{1}{\epsilon_1} + D\left(\dfrac{1}{\epsilon_2} - 1\right) - \dfrac{4}{3} D\left(\dfrac{\ln D}{1-D}\right)\rho_{12}}, \tag{30}$$

$$\theta^4 = \frac{\dfrac{4}{3\epsilon_2} - \dfrac{2}{3} - \rho_2\ln\left(\dfrac{\rho}{\rho_2}\right)}{\dfrac{4}{3\epsilon_2} - \dfrac{4}{3} + \dfrac{4}{3\epsilon_1 D} - \dfrac{\ln D}{(1-D)}\rho_{12}}. \tag{31}$$

Equations (30) and (31) are applicable for all values of D.

For the case with internal heat generation ($\theta_G = 1.0$), a similar argument can be applied. The existing approximate results[10] for the planar, one-dimensional problem suggest that the temperature profile can be closely approximated by

$$\theta^4 = \lambda(\rho) + \beta(\rho)(\rho - \rho_m)^2. \tag{32}$$

Combining the heat-flux boundary conditions at the two cylinder surfaces and at the interface between adjacent infinitesimal cylindrical gas elements yields the following analogous relation to eqn (22):

$$-\frac{4}{3\epsilon_2}\rho_{12}\beta_n + \frac{4}{3}\rho_{12}\beta_n + \frac{4}{3}\frac{\rho_{12}}{\epsilon_1}\beta_1$$

$$= \lambda_n - \lambda_1 + (\beta_n - \beta_1)\frac{\rho_{12}^2}{4} + \frac{4}{3}\int_{\rho_1}^{\rho_2}\beta(\rho')\,d\rho'. \tag{33}$$

where $\lambda_n = \lambda(\rho_2)$, $\lambda_1 = \lambda(\rho_1)$, $\beta_n = \beta(\rho_2)$ and $\beta_1 = \beta(\rho_1)$. Applying the temperature-continuity condition and the conservation of energy, two differential equations in terms of $\lambda(\rho)$ and $\beta(\rho)$ can again be obtained. They are

$$\frac{d\lambda}{d\rho} + \frac{d\beta}{d\rho} (\rho - \rho_m)^2 = 0,$$ (34)

$$\frac{d}{dr}\left[-\frac{8}{3}\beta(\rho)(\rho - \rho_m)r \right] = r.$$ (35)

Solution of eqns (34) and (35) gives

$$\lambda(\rho) = \lambda_n - \frac{3}{16}\rho_m(\rho - \rho_2) + \left(\rho_{12}\beta_n\rho_2 + \frac{3}{8}\rho_2^2\right)\left(\ln\frac{\rho}{\rho_2} + \frac{1}{2}\frac{\rho_n}{\rho} - \frac{1}{2}\frac{\rho_m}{\rho_2}\right),$$ (36)

$$\beta(\rho) = \frac{\frac{\rho_{12}}{2}\rho_2\beta_n + \frac{3}{16}(\rho_2^2 - \rho^2)}{\rho(\rho - \rho_m)}.$$ (37)

Substituting eqns (36) and (37) into eqn (33), the solution for β_n can be easily obtained as follows:

$$\beta_n = \frac{3}{8}(1+D)\frac{\frac{1}{\epsilon_1 D} + \frac{\ln D}{(1+D)^2(1-D)} - \frac{1}{2(1+D)} - \frac{3\rho_{12}\ln D}{4(1-D)^2(1+D)} - \frac{3}{8}\frac{\rho_{12}}{1-D}}{\frac{1}{\epsilon_2} - 1 + \frac{1}{\epsilon_1 D} + \frac{\ln D}{1+D} - \frac{3\rho_{12}\ln D}{4(1-D)}}.$$ (38)

Equation (38), together with the heat-flux boundary condition at the outer cylinder represented by eqn (17), leads to the following expression for λ_n:

$$\lambda_n = \beta_n\left[-\frac{\rho_{12}^2}{4} - \frac{4}{3\epsilon_2}\rho_{12} + \frac{2}{3}\rho_{12} - 1 \right].$$ (39)

Physically, the most interesting quantity for the concentric-cylinders problem with internal heat generation is the fractional heat loss to the outer cylinder defined by

$$\Phi = \frac{q_r(r_2)2\pi r_2}{\pi(r_2^2 - r_1^2)}.$$ (40)

Utilizing eqns (38) and (39), Φ can be written explicitly as

$$\Phi = \frac{\frac{1}{\epsilon_1 D} + \frac{\ln D}{(1+D)^2(1-D)} - \frac{1}{2(1+D)} - \frac{3\rho_{12}\ln D}{4(1-D)^2(1+D)} - \frac{3}{8}\frac{\rho_{12}}{(1-D)}}{\frac{1}{\epsilon_2} - 1 + \frac{1}{\epsilon_1 D} + \frac{\ln D}{1+D} - \frac{3\rho_{12}\ln D}{4(1-D)}}.$$ (41)

The dimensionless temperature profile within the enclosure becomes

$$\theta^4 = \frac{3}{8}(1+D)\Phi\left[\frac{4}{3\epsilon_2}\rho_{12} - \frac{2}{3}\rho_{12} + 1 - \rho_{12}\rho_2\ln\frac{\rho}{\rho_2}\right]$$
$$+ \frac{3}{8}\left[\rho_2^2\ln\frac{\rho}{\rho_2} + \frac{1}{2}(\rho_2^2 - \rho^2)\right].$$ (42)

As for the case without internal heat generation, eqn (41) and (42) are applicable for all values of D.

Radiative transfer between two concentric spheres

Following the same argument as in the previous section, an approximate solution for the radiative transfer problem between two concentric spheres may be obtained. In fact, every equation in the previous section can be applied to the concentric-spheres problem with the exception of the energy-conservation relations. for the case without internal heat generation ($\theta_G = 0$), eqn (25) is replaced by

$$\frac{d}{dr}\left[-\frac{4}{3}\beta(\rho)r^2 \right] = 0.$$ (43)

For the case with internal heat generation ($\theta_G = 1.0$), eqn (35) becomes

$$\frac{d}{dr}\left[-\frac{8}{3}\beta(\rho)(\rho - \rho_m)r^2\right] = r^2.$$ (44)

Because of its obvious similarity to the concentric-cylinders problem, the algebraic detail of the calculation for the concentric-spheres problem will not be presented.

The heat loss from the inner sphere and the temperature profile for the case with no internal heat generation are given by

$$q_r(r_1) = \frac{1}{D^2\left(\frac{1}{\epsilon_2} - 1\right) + \frac{1}{\epsilon_1} + \frac{3}{4}D\rho_{12}},$$ (45)

$$\theta^4 = \frac{\frac{1}{\epsilon_2} - \frac{1}{2} + \frac{3}{4}\rho_2\left[\frac{\rho_2}{\rho} - 1\right]}{\frac{1}{\epsilon_2} - 1 + \frac{1}{\epsilon_1 D^2} + \frac{3}{4}\frac{\rho_{12}}{D}}.$$ (46)

For the case with internal heat generation ($\theta_G = 1.0$), the fractional heat loss to the outer sphere and the temperature profile become

$$\Phi = \frac{q_r(r_2)4\pi r_2^2}{4/3\pi(r_2^3 - r_1^3)}$$

$$= \frac{\frac{2\ln D}{(1-D^3)(1+D)^2} - \frac{(1-\frac{1}{2}D-\frac{1}{2}D^3)}{D(1+D)(1-D^3)} + \frac{1}{\epsilon_1 D^2} + \frac{3\rho_{12}(2+D)}{8D(1+D+D^2)}}{\frac{2\ln D}{(1+D)^2} - \frac{(1+D^2)}{D(1+D)} + \frac{1}{\epsilon_2} + \frac{1}{\epsilon_1 D^2} + \frac{3}{4}\frac{\rho_{12}}{D}},$$ (47)

$$\theta = \frac{1}{4}(1+D+D^2)\Phi\left[\frac{4}{3\epsilon_2}\rho_{12} - \frac{2}{3}\rho_{12} + \rho_{12}\rho_2\left(\frac{\rho_2}{\rho} - 1\right) + 1\right] + \frac{3}{8}\rho_2^2 - \frac{1}{4}\frac{\rho_2^3}{\rho} - \frac{1}{8}\rho^2$$ (48)

As for the concentric-cylinders problem, eqns (45)–(48) are applicable for all values of D.

4. RESULTS AND DISCUSSION

Heat-flux results based on eqns (30), (41), (45) and (47) are illustrated in Figs. 3–8. Some typical temperature profiles based on eqns (31), (42), (46) and (48) are presented in Figs. 9–16. Exact solutions, if available, are presented together with the approximate result to demonstrate the effectiveness of the present approximation.

Comparisons show that the approximate heat flux is generally quite accurate for all values of D, ρ_{12} and ϵ (for simplicity, the two surfaces are assumed to have the same emissivity of ϵ). Unlike results of existing approximation techniques, our heat-flux prediction reduces to the correct result in the optically thin limit. The accuracy of the temperature profile, on the other hand, is less satisfactory. It shows the same difficulty as the various traditional approximation techniques[4,10] for the planar problem. Approximate results for the gas temperature near the two boundaries are not very accurate. But the accuracy improves as the optical thickness increases.

Some useful physical information concerning the two non-planar radiative transfer problems may be derived from the results shown in Figs. 3–16. Some of these conclusions have also been obtained by other investigators.[8,9] Figure 3 shows the heat transfer between concentric black cylinders and concentric black spheres without internal heat generation. The results show the familiar trend of decreasing heat transfer with increasing optical thickness. In the optically thick limit, the present approximation gives the following heat flux expressions for the two non-planar geometries:

$$q_r(r_1) \xrightarrow[\rho_{12}\to\infty]{} \frac{3(D-1)}{4D\ln D\rho_{12}} \quad \text{for concentric cylinders,}$$ (49)

and

$$q_r(r_1) \xrightarrow[\rho_{12}\to\infty]{} \frac{3}{4D\rho_{12}} \quad \text{for concentric spheres,}$$ (50)
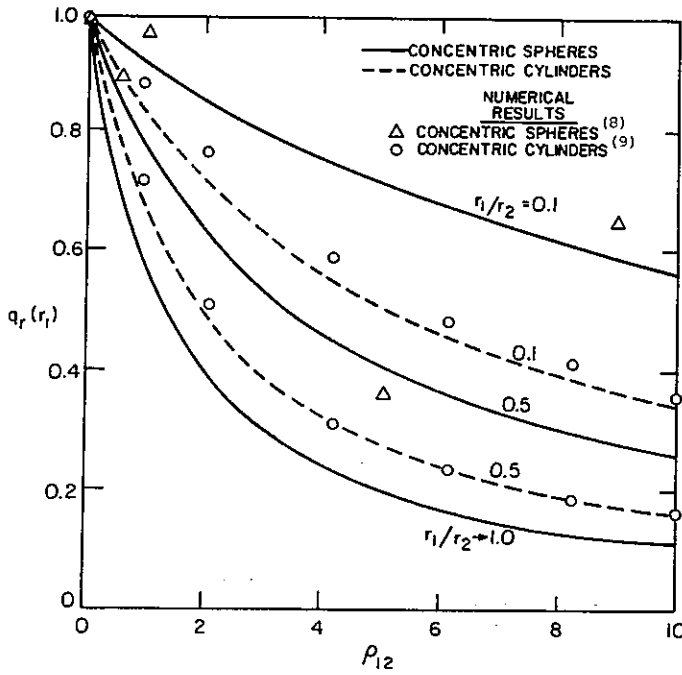
Fig. 3. Effect of radius ratio on heat-transfer results for the one-dimensional, non-planar problem with no heat generation.
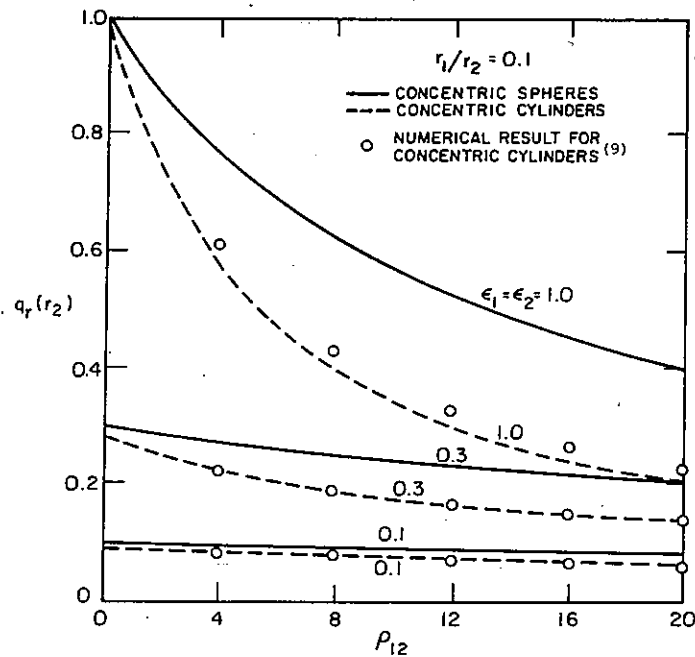

Fig. 4. Effect of the wall emissivity on the heat-transfer result for the one-dimensional. non-planar problem with no heat generation.

It is interesting to observe that the above approximate limiting heat-flux expressions give the same $1/p_{12}$ dependence as various approximate heat-flux expressions for the one-dimensional planar problem. There results suggest that, in the optically-thick limit, radiative heat transfer in non-planar enclosures does not differ significantly from the planar case. The non-planar geometry introduces only a constant multiplicative factor on the optically-thick limiting heat-flux expression.

In the optically-thin unit, the heat-flux expressions represented by eqns (30) and (48) are
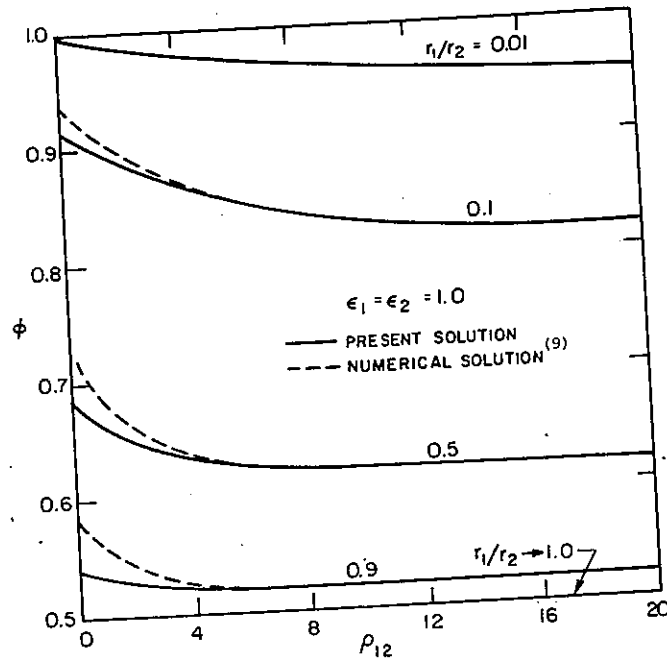
Fig. 5. Fractional heat loss to the outer cylinder for the concentric-cylinders problem with heat generation.
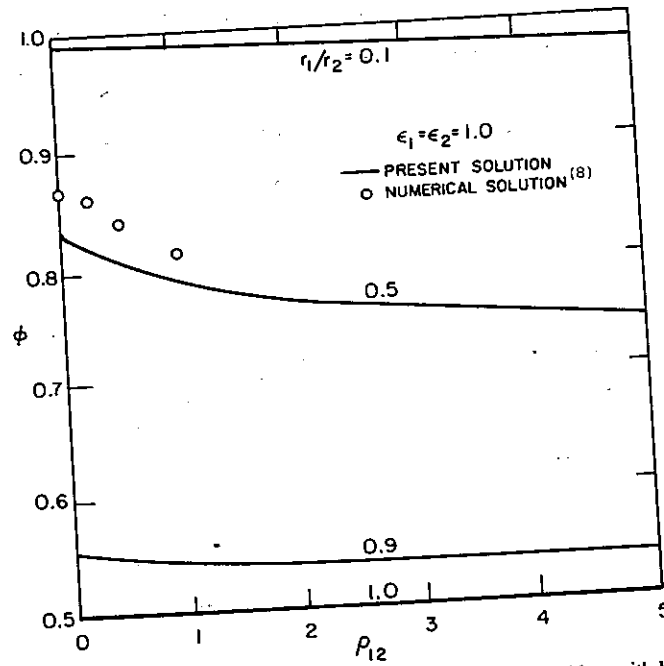
Fig. 6. Fractional heat loss to the outer sphere for the concentric-spheres problem with heat generation.

reduced to

$$q_r(r_1) \xrightarrow[\rho_{12} \to 0]{} \frac{1}{1/\epsilon_1 + D\left(\dfrac{1}{\epsilon_2} - 1\right)} \quad \text{for concentric cylinders} \tag{51}$$
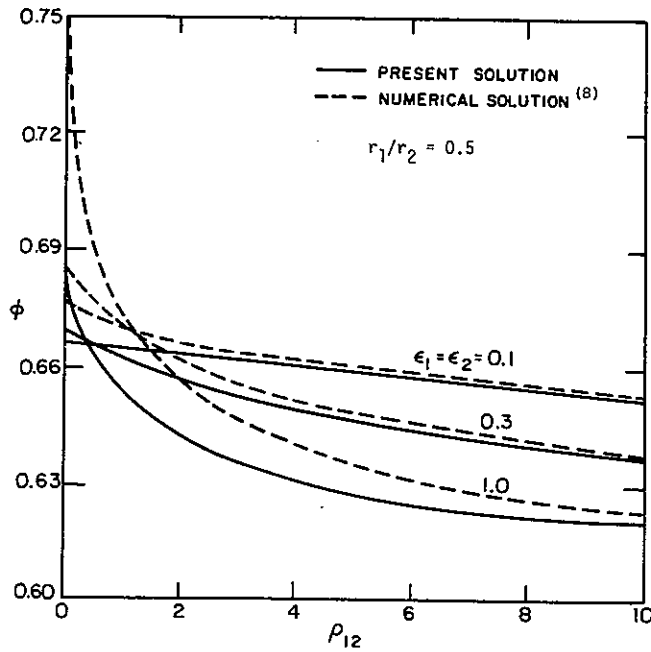
and

$$q_r(r_1) \xrightarrow[\rho_{12} \to 0]{} \frac{1}{1/\epsilon_1 + D^2\left(\dfrac{1}{\epsilon_2} - 1\right)} \quad \text{for concentric spheres.} \tag{52}$$

Fig. 7. Effect of wall emissivity on the fractional heat loss to the outer cylinder for the concentric-cylinders problem with heat generation.
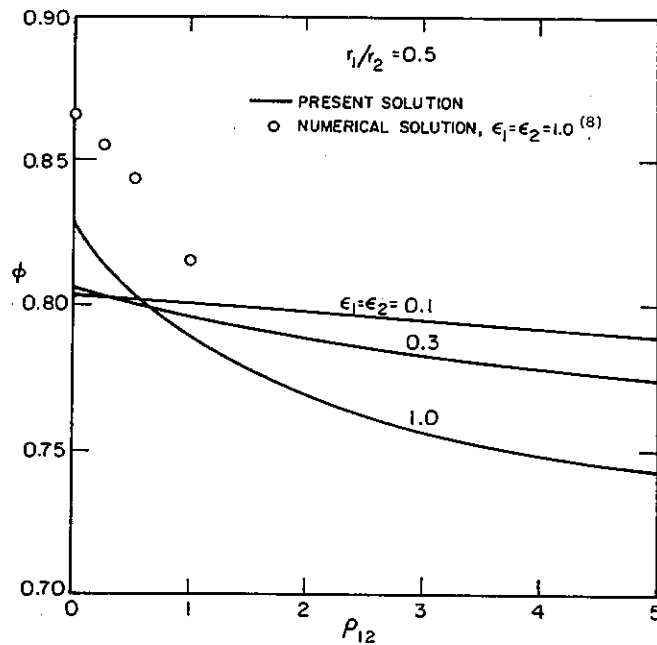

Fig. 8. Effect of wall emissivity on the fractional heat loss to the outer sphere for the concentric-spheres problem with heat generation.

It is interesting to note that these expressions are in agreement with the well known solutions for radiative exchange with no participating medium in concentric cylindrical and concentric spherical enclosures.[11]

Figure 3 also illustrates the effect of the radius ratio D on the heat-transfer result for non-planar systems. Results show that, for both non-planar cases, a decrease in the radius ratio increases the heat transfer. Physically, this phenomenon can be explained by observing that the energy emitted by the inner surface can be partially reabsorbed because of the radiative absorption and re-emission by the enclosed gas. The amount of energy reabsorbed by the inner surface depends on the area ratio between the inner and the outer surfaces. In terms of the
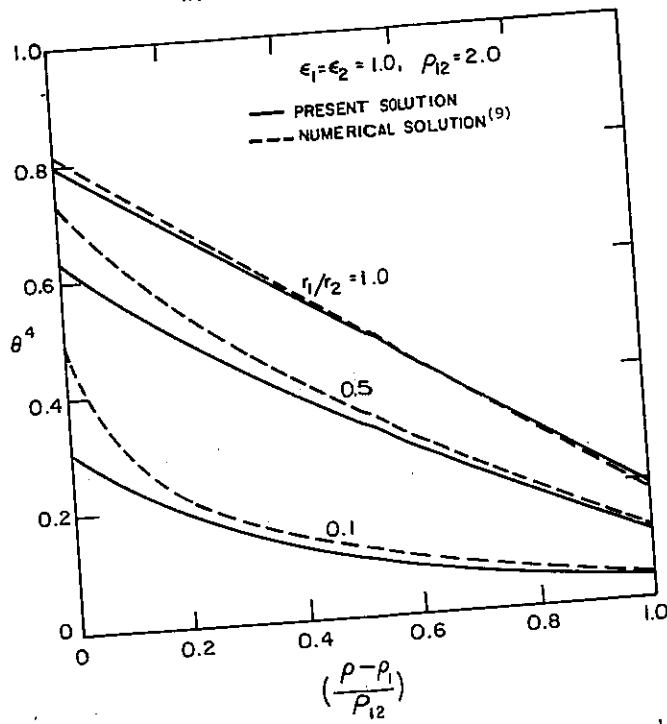
Fig. 9. Effect of radius ratio on the temperature profile for the concentric-cylinders problem with no heat generation.
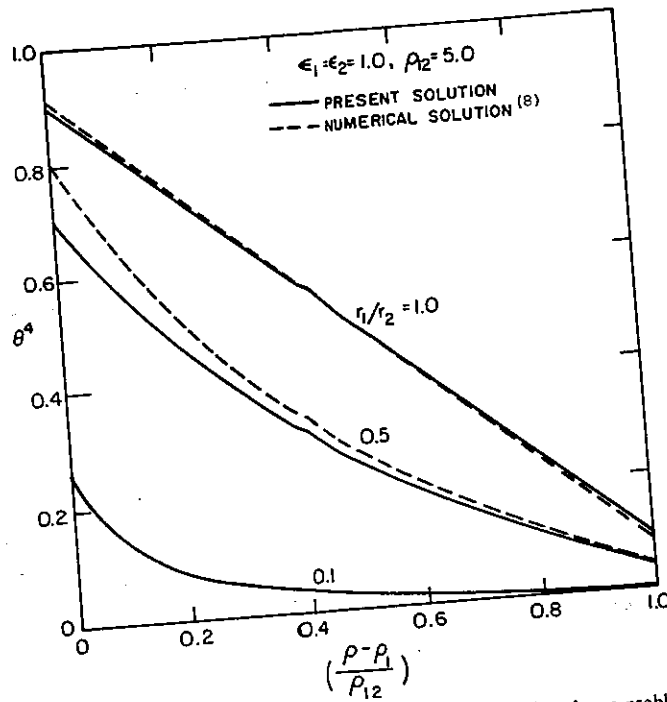

Fig. 10. Effect of radius ratio on the temperature profile for the concentric-spheres problem with no heat generation.

radius ratio D, area ratios for the two non-planar systems considered here are given by

$$A_s = D^2 \quad \text{for concentric sphere,} \tag{53}$$

$$A_c = D \quad \text{for concentric cylinder.} \tag{54}$$

In both cases, a small radius ratio indicates a small area ratio. Only a small amount of the
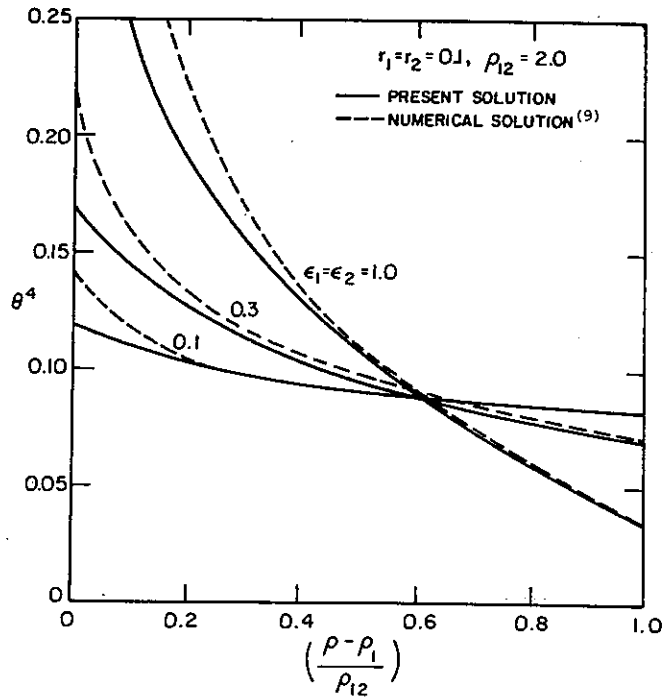
Fig. 11. Effect of wall emissivity on the temperature profile for the concentric-cylinders problem with no heat generation.
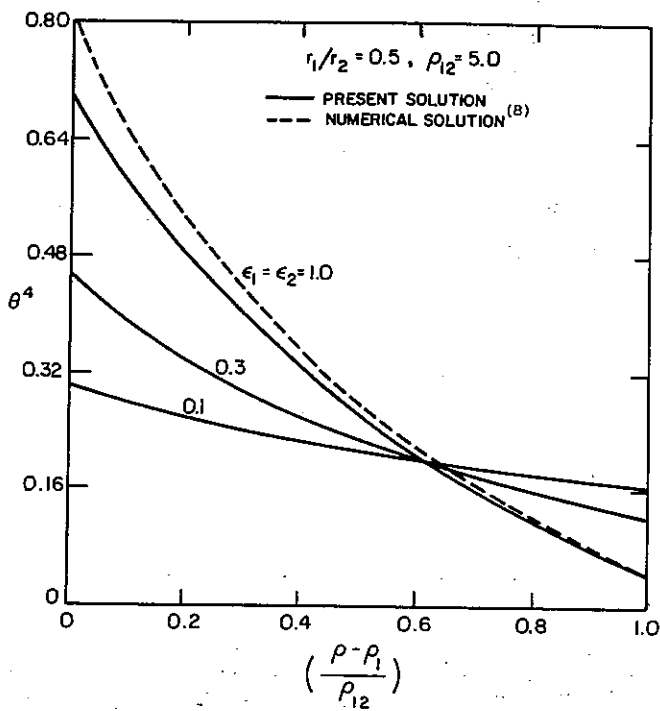

Fig. 12. Effect of wall emissivity on the temperature profile for the concentric-spheres problem with no heat generation.

energy emitted by the inner surface can be reabsorbed. The heat transfer is thus large for small value of D and $q_r(r_1) \to 1.0$ as $D \to 0$. As D increases, the area ratio also increases and more energy can be reabsorbed by the inner surface. The heat transfer is less and approaches the planar solution in the limit of $D \to 1.0$.

Results in Fig. 3 also show that, for fixed values of D and ρ_{12}, heat transfer between two
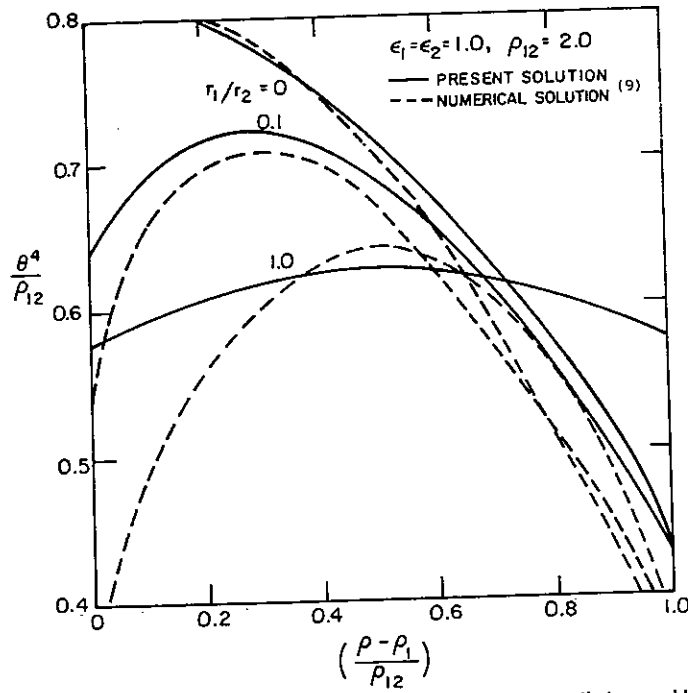
Fig. 13. Effect of radius ratio on the temperature profile for the concentric-cylinders problem with heat generation.
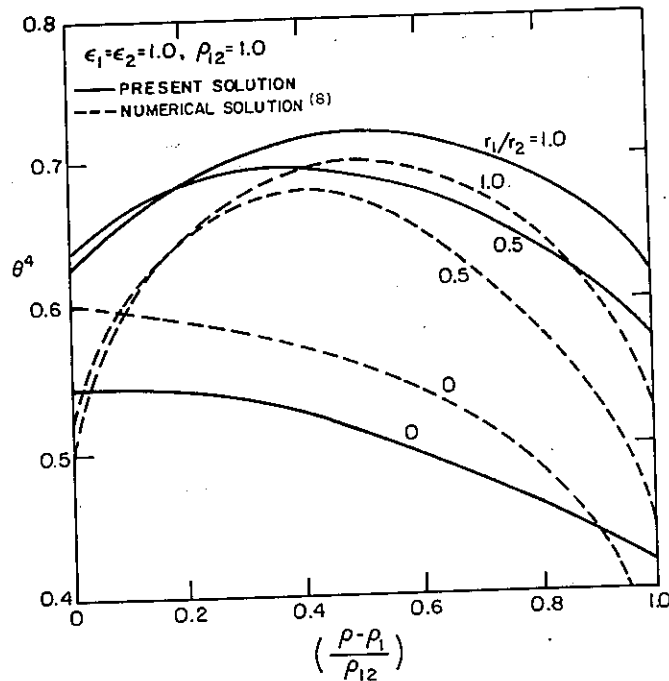

Fig. 14. Effect of the radius ratio on the temperature profile for the concentric-spheres problem with uniform heat generation.

concentric spheres is larger than that between two concentric cylinders. This can be explained by noting that, from eqns (53) and (54), A_s is less than A_c for a given set of values for D and ρ_{12}. The extent of the inner surface in a concentric spherical enclosure is effectively less than that in a concentric cylindrical enclosure. The reabsorption effect described above is thus small and heat transfers more readily in a concentric spherical enclosure.

The effect of wall emissivity on the heat-transfer result for the case with no internal heat
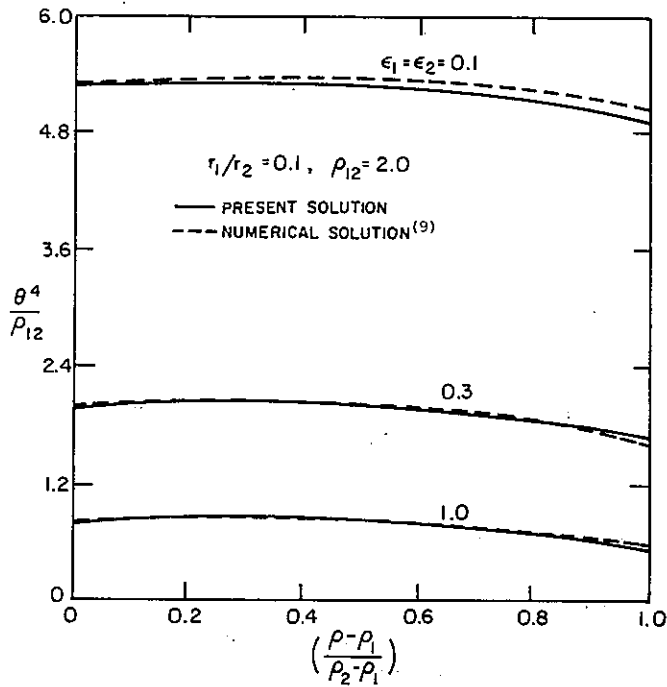
Fig. 15. Effect of wall emissivity on the temperature profile for the concentric-cylinders problem with heat generation.
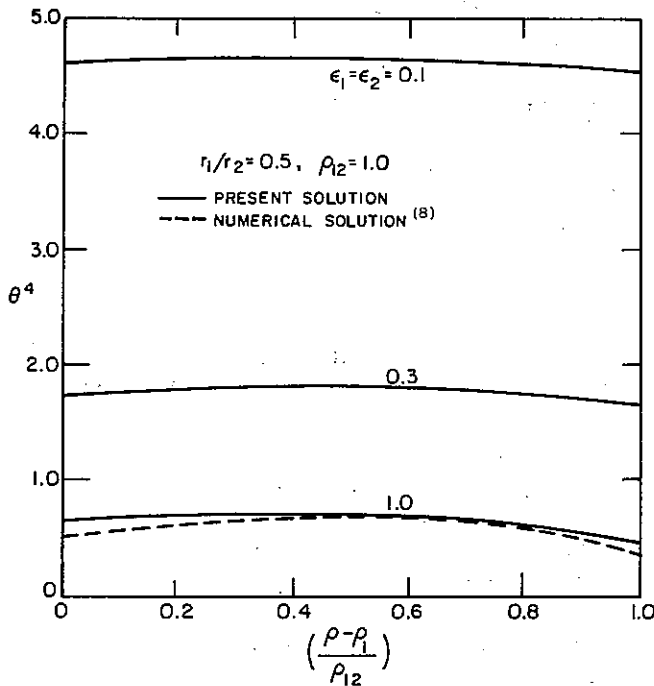

Fig. 16. Effect of emissivity on the temperature profile for the concentric-spheres problem with uniform heat generation.

generation is illustrated in Fig. 4. Physically, a decrease in the wall emissivity means that a larger fraction of the energy emitted by the inner surface can be reabsorbed because of reflection by the outer surface. Heat transfer therefore decreases as the wall emissivity decreases. For small emissivities, these reflection and reabsorption processes become dominant and heat transfer becomes relatively independent of the optical thickness.

Figures 5 and 6 show the heat transfer result for the case with internal heat generation and zero wall temperature. These results indicate that, for both non-planar cases, the fractional heat

loss to the outer surface. Φ, in the optically-thick limit is only a function of the enclosure geometry and is independent of the optical thickness. Utilizing eqns (41) and (47), these limiting expressions are given by

$$\Phi \xrightarrow[\rho_{12}\to\infty]{} \frac{1}{(1-D^2)} + \frac{1}{2\ln D} \quad \text{for concentric cylinders} \tag{55}$$

and

$$\Phi \xrightarrow[\rho_{12}\to\infty]{} \frac{(2+D)}{2(1+D+D^2)} \quad \text{for concentric spheres.} \tag{56}$$

Physically, the above result is not too surprising because, in the optically thick limit, radiative heat transfer becomes a local phenomenon. As for heat conduction, the heat-loss distribution to the two bounding surfaces depends only on the enclosure geometry. As the optical thickness decreases, the radiative effect becomes non-localized. The heat-loss distribution becomes more dependent on the optical thickness. Results show that the fractional heat loss to the outer surface increases because the larger outer surface can be more readily seen by the enclosed gas.

Results in Figs. 5 and 6 also illustrate some interesting effects of the radius ratio D on the heat-transfer result. As the radius ratio decreases, the fractional heat loss to the outer surface increases because of the effective decrease in the area of the inner surface. In the limit of $D\to0$, all of the heat generated within the enclosure is absorbed by the outer surface because of the small inner surface area. In the limit of $D\to1.0$, the non-planar problem reduces to the planar case. An equal amount of energy is transferred to each surface. It is interesting to observe that, for a given set of values of D and ρ_{12}, the results in Figs. 5 and 6 show that the fractional heat loss to the outer surface of a concentric spherical enclosure is larger than that of a concentric cylindrical enclosure. This phenomenon can again be explained by noting the difference between the area ratio of the concentric cylindrical enclosure and that of the concentric spherical enclosure. Since A_s is less than A_c, the outer surface of a concentric spherical enclosure represents a larger fraction of the total surface area than that of a concentric cylindrical enclosure. The enclosed gas is exposed to more of the outer surface in a concentric spherical enclosure. Heat loss to the outer surface is thus larger.

Figures 7 and 8 demonstrate the effect of the emissivity on the heat-transfer result with internal heat generation. It is interesting to observe that, for a small optical thickness, a decrease in the emissivity reduces heat loss to the outer surface. The opposite behavior is observed for an enclosure with a large optical thickness. This result obtains because, physically, a small optical thickness represents small gas absorption. The energy generated within the enclosure goes directly to the two bounding surfaces. The energy reflected by the inner surface is partially absorbed by the outer surface while the energy reflected by the outer surface is partially absorbed by the inner surface. But, as may readily be shown by a simple "image" analysis, the net result of these multiple reflections is an increase in the heat loss to the inner surface. A decrease in the emissivity thus reduces heat loss to the outer surface. A large optical thickness, on the other hand, represents large gas absorption. The energy reflected by the two walls is mainly absorbed and reemitted by the gas. Since the gas is in more direct contact with the outer surface, a majority of this reflected energy is reabsorbed by the outer surface. Heat transfer to the outer surface thus increases with decreasing wall emissivity when the optical thickness is large.

The effect of the radius ratio on the gas temperature for the case with no internal heat generation is shown in Figs. 9 and 10. As D decreases, the gas temperature decreases because the gas is influenced more by the cold outer surface. For given values of D and ρ_{12}, the gas temperature in a concentric spherical enclosure is lower than that in a concentric cylindrical enclosure, again because there are proportionally more outer surface areas in a concentric spherical enclosure.

The effect of wall emissivity on the gas temperature for the case with no heat generation is shown in Figs. 11 and 12. The result presents no surprises. The multiple reflections of the radiant energy by the two bounding walls smooth out the temperature profile as the wall emissivity decreases.

For the case with internal heat generation, the effect of the radius ratio on the gas temperature is illustrated by Figs. 13 and 14. In the limit of $D \to 1.0$, the temperature profile is reduced to that of the parallel-plate case and is symmetric about the midpoint between the two surfaces. When $D < 1.0$, the area of the outer surface is larger than that of the inner surface. The energy generated at the region near the outer surface is released more easily to the adjacent boundary than the energy generated near the inner surface. The gas temperature near the inner surface is therefore high while the gas temperature near the outer surface is low. These results explain the temperature-profile behavior shown in Figs. 13 and 14.

Finally, Figs. 15 and 16 demonstrate the effect of wall emissivity on the gas temperature for the case with internal heat generation. As the wall emissivity decreases, the gas temperature increases because higher gas emission is needed to release the constant amount of energy generated within the enclosure. As for the case with no heat generation, the temperature distribution is more uniform because of multiple reflections of radiant energy by the two boundaries.

5. CONCLUSION

Utilizing results of existing approximations for the one-dimensional planar problem, closed-form expressions are derived for the heat transfer and temperature profiles for the one-dimensional, non-planar problem. These expressions compare favorably with available numerical solutions. The heat-flux expression is shown to be accurate for all values of the optical thickness. The temperature-profile expressions are also quite accurate, except at the region near the two boundaries.

The optical thickness, the surface emissivity and the radius ratio are shown to have some interesting and significant effects on the heat-transfer and temperature profiles for the one-dimensional, non-planar problem. The radiative heat transfer characteristic of a concentric spherical enclosure and those of a concentric cylindrical enclosure are found to exhibit some interesting differences because of geometric differences between the two enclosures.

REFERENCES

1. R. D. CESS, Z. AGNEW. *Math. Phys.* **17**, 776 (1966).
2. M. A. HEASLET and R. F. WARMING. *JQSRT* **5**, 669 (1965).
3. M. A. HEASLET and R. F. WARMING. *JQSRT* **6**, 751 (1966).
4. R. G. DEISSLER, *J. Heat Transfer* **C86**, 220 (1964).
5. Y. S. CHOU and C. L. TIEN. *JQSRT* **8**, 919 (1968).
6. E. A. DENNAR and M. SIBULKIN. *J. Heat Transfer* **C91**, 73 (1969).
7. I. L. RYHMING. *Int. J. Heat Mass Transfer* **9**, 315 (1966).
8. E. M. SPARROW, C. M. USISKIN and H. A. HUBBARD. *J. Heat Transfer* **C83**, 240 (1961).
9. M. PERLMUTTER and J. R. HOWELL. *J. Heat Transfer* **C86**, 169 (1964).
10. W. W. YUEN and C. L. TIEN. A differential formulation of radiative transfer with multi-moment boundary conditions. *J. Heat Transfer*, to be published.
11. R. SIEGEL and J. R. HOWELL. *Thermal Radiation Heat Transfer*. McGraw-Hill, New York (1972).